16th ICAAR LISBOA 2020-2022

16th International Conference on
Alkali-Aggregate Reaction in Concrete
Lisboa | LNEC | Portugal | 31 May - 2 June 2022

http://icaar2020-2022.lnec.pt

Residual load carrying capacity of ASR damaged reinforced concrete beam after 12 years exposure

Susumu Inoue

Osaka Institute of Technology, Osaka, Japan, susumu.inoue@oit.ac.jp

Abstract

After the reports on the rupture of stirrups and longitudinal steels in T-shaped beams of bridge piers mainly due to ASR expansion, concentrated research works had been done in Japan. Based on these researches, it is generally recognized that residual load carrying capacity of ASR damaged members with ruptured steels can be estimated considering appropriately the anchorage length of ruptured steels as far as the bond between concrete and reinforcing steels is guaranteed. However, it is important to make clear the load carrying mechanism of ASR damaged members after a long time exposure.

At the 14th ICAAR, the author reported on the effect of rupture of stirrups on load carrying behaviour of ASR damaged beams. In that case, however, the discussions were mainly based on the test results of relatively small specimens (300mm- square cross section) after the exposure of approximately 1.5 and 3 years.

In this paper, load carrying behaviour of an ASR damaged reinforced concrete beam with a relatively large cross section (600mm-square) after 12 years exposure (ASR expansion almost finished) is discussed. The specimen was cut into 3 pieces after the loading test at the positions where the effect of loading test could be eliminated, and expansive crack propagation inside the concrete was observed. In addition, the effect of anisotropy of ASR expansion on the mechanical properties of inner concrete is examined by using concrete core specimens.

Test results indicated that the residual capacity of the ASR damaged beam well exceeded the design value because the rupture of stirrups did not occur during the exposure period. In addition, compressive strength of core concrete was affected by the anisotropy of ASR expansion.

***Keywords**: anisotropy of expansion; ASR damage; compressive strength; crack propagation; residual capacity*

1. INTRODUCTION

In the last two decades, vigorous research works have been done on the structural effects of ASR expansion, for example, by Multon et al. [1]. While in Japan, it was reported in the early years of the 21st century that stirrups, as well as longitudinal steels, in T-shaped beams of reinforced concrete bridge piers were ruptured at the bent corner or butt joints. In order to make clear the causes of this rupture, concentrated researches had been done after the finding of the rupture in existing reinforced concrete structures. These researches concluded that this phenomenon occurred not only due to excessive ASR expansion but also under complex combinations of several factors, such as mechanical properties and surface shape of reinforcing bars, bending or welding methods of reinforcing bars, corrosive atmospheres and so on [2]. As for the load carrying capacity of ASR damaged structures, on the other hand, it is indicated that in most cases structural safety of damaged members is guaranteed at the present stage as far as the anchorage of ruptured steels is maintained by the bond between concrete and reinforcing bars, based on the site inspections of the damaged structures as well as some experimental and analytical investigations [2].

The author also reported on the residual shear capacity of ASR damaged reinforced concrete beams with ruptured stirrups at the 13th [3] and 14th ICAAR [4]. The main conclusions of these studies are as follows. 1) The introduced chemical prestress due to ASR expansion increased the concrete shear capacity. This positive effect was rather larger compared with the negative effect of the deterioration in material properties. 2) As for the effects of rupture of stirrups, the ruptured stirrups could not effectively restrain the ASR expansion in vertical direction and the dowel force of the longitudinal bars at the shear cracks, resulting in the significant propagation of the shear bond cracks along with the longitudinal bars.

Such shear bond cracks might lead to the premature shear bond failure even when the ruptured stirrups carried some parts of the applied shear force just before the failure.

However, these were based on the test results of relatively small specimens after the exposure of up to 3 years. In addition, rupture of stirrups was imitated by cutting the bent corner of them beforehand. Therefore, it is important to examine whether rupture of stirrups occurs in the beam during long-time exposure. Information on residual capacity after long-time exposure as well as the effect of anisotropic expansion in concrete structures on mechanical properties of concrete is also useful for rational countermeasures against ASR damaged structures.

In this paper, load carrying behaviour of an ASR damaged reinforced concrete beam with a relatively large cross section (600mm-square) is discussed. This specimen was exposed to natural outside condition for almost 12 years. After the loading test, this specimen was cut into 3 pieces at the positions where the effect of loading test could be eliminated, and expansive crack propagation inside the concrete was observed. In addition, the effect of anisotropy of ASR expansion on the mechanical properties of internal concrete is examined by using concrete core specimens.

2. OUTLINE OF TESTS

The specimen used was a reinforced concrete beam with width x full depth x total length of 600 x 600 x 4000mm as shown in Figures 2.1 and 2.2. Sixteen D22 reinforcing bars (f_{sy}=385N/mm^2) were used for longitudinal reinforcement (tensile reinforcement ratio p=1.99%) and D13 stirrups (f_{sy}=328N/mm^2) were used for shear reinforcement (shear reinforcement ratio p_w=0.40%). This beam was designed to fail in shear in order to evaluate the effectiveness of stirrups within ASR damaged concrete. Two kinds of bending radius for stirrups, 2.0ϕ and 1.0ϕ (ϕ: bar diameter), were selected in order to examine the effect of bending radius on the rupture of stirrups during exposure period. This is because many of the practically ruptured stirrups had smaller bending radius less than 2.0ϕ. The design compressive strength of concrete was 24N/mm^2. The mix proportion of used reactive concrete is shown in Table 2.1, in which that of non-reactive normal concrete (N) is also indicated for comparison. Reactive fine and coarse

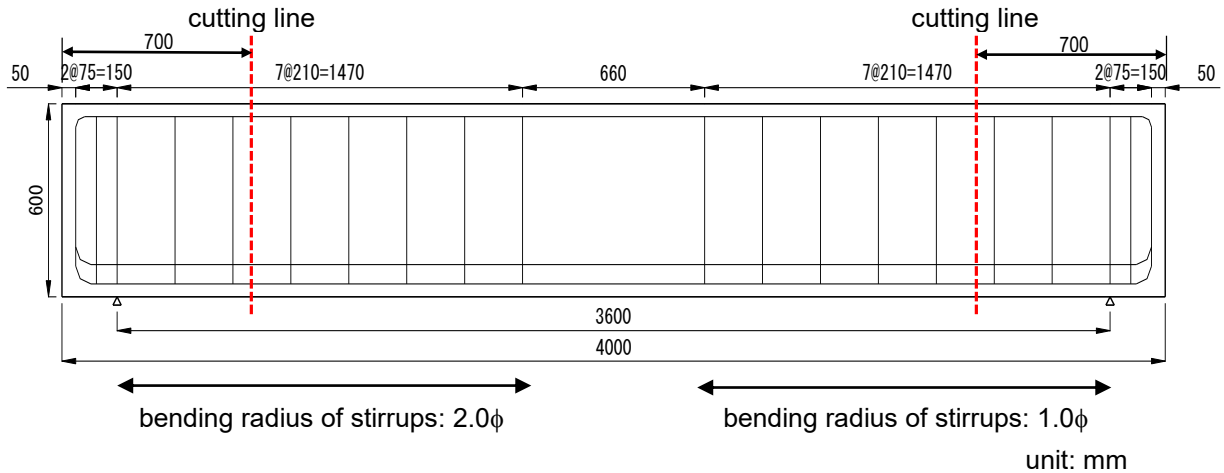

Figure 2.1: Reinforcing details of specimen

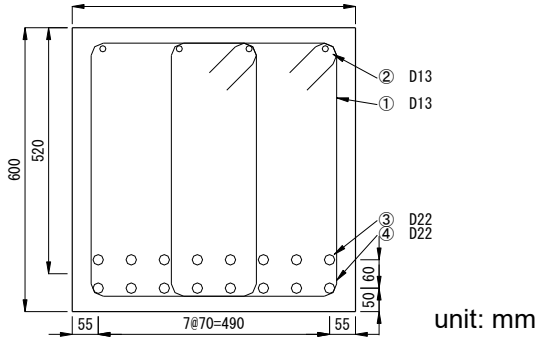

Figure 2.2: Cross section

aggregates, which are categorized as one of andesite and judged as “not harmless” by JIS A 1145 “Method of test for alkali-silica reactivity of aggregates by chemical method” [5], were used in the pessimum (approximately 50% by weight) for the concrete. Sodium chloride (NaCl) was also added so that the total alkali contents might become 8kg/m^3.

Table 2.1: Mix proportions of concrete

Type	G_{max} (mm)	Slump (cm)	Air (%)	W/C (%)	s/a (%)	Unit weight (kg/m^3)							Water Reducing Agent (cc/m^3)
						W	C	S normal	S reactive	G normal	G reactive	NaCl	
N	25	12	4.5	63	45.8	183	290	840	-	1080	-	-	726
ASR	25	12	4.5	63	45.8	183	290	394	411	507	492	13.1	726

This beam was exposed to outside natural environment but off the ground for 4495 days (more than 12 years) after casting of concrete as shown in Figure 2.3. During the exposure, it was simply supported and subjected to the stress caused by its own weight. During the last 5 years of exposure, the temperature range was -4.8 to 39.6 degree centigrade and the average was 16.4 degree centigrade, while the average relative humidity was about 72.5%. During the exposure, changes in the vertical, horizontal and longitudinal strain of the concrete surface and ultrasonic pulse velocity were measured in addition to the observation of crack propagation.

Figure 2.3: Exposed specimen (at the age of 1.5 years)

After the exposure, the beam was loaded monotonously up to failure under symmetrical two-point loads (shear span: 990mm, flexural span: 1520mm). The shear span - effective depth ratio (a/d) was set as 1.9 so that the effect of shear force might become dominant. During the loading test, applied load, deflections at the mid span and the loading points were recorded. In addition, the propagation of cracks during loading was observed.

3. RESULTS AND DISCUSSIONS

3.1 Expansion characteristics during exposure period

3.1.1 Expansion characteristics

Figure 3.1 shows the expansive crack profiles after the exposure of 491 and 4495 days. As seen in this figure, the density of expansive cracks in the upper and side surfaces, as well as the width of existing cracks, increased during this period. In addition, longitudinal cracks along with the tensile reinforcement developed remarkably.

Figure 3.2 shows the changes in concrete strain used for the beam, in which the values of non-reactive normal concrete having the same W/C ratio are also indicated for comparison. These strains were measured using 100 x 100 x 400mm concrete prisms exposed to the same environment as the beam specimen. Figure 3.3 shows the changes in concrete surface strain of the beam, in which the horizontal

strain in the upper surface, the vertical ones in the side surfaces and the longitudinal ones (upper: 80mm from the top fibre, lower: 80mm from the bottom fibre) in the side surfaces are indicated. All of these values are the average ones obtained from several measuring points. Although no measurement was

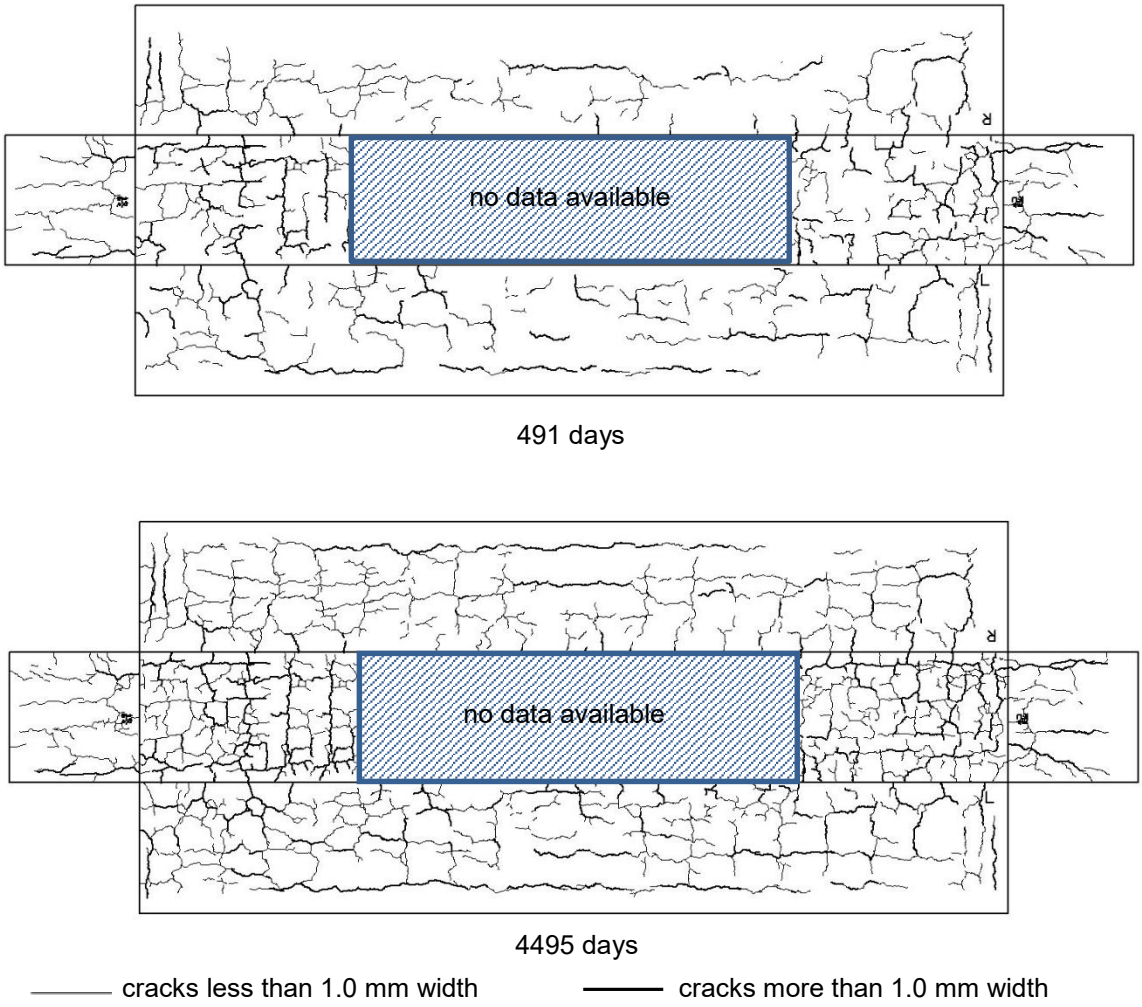

Figure 3.1: Expansive cracking patterns of the beam

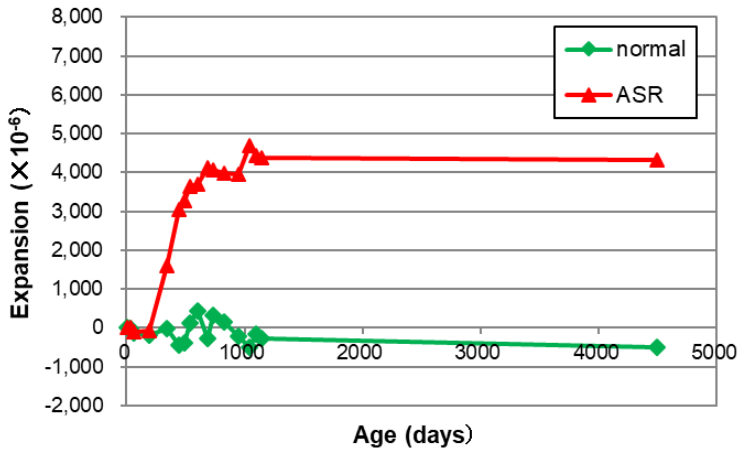

Figure 3.2: Changes in expansive strain of used concrete

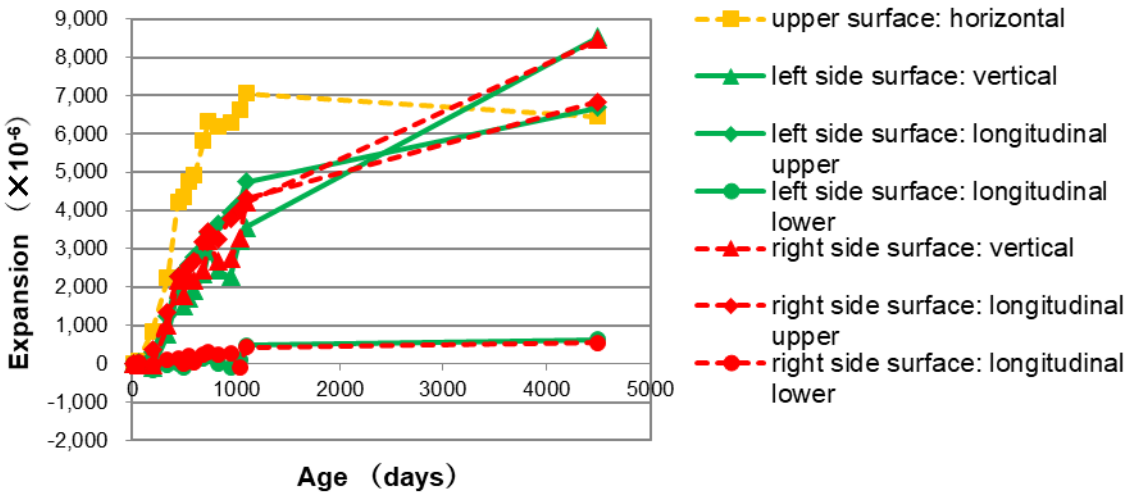

Figure 3.3: Expansion of concrete surface of the beam

done between 3 and 12 years, the accuracy of the measured values after 12 years exposure was guaranteed because these values were calculated from the elongations measured mechanically between two contact tips embedded in the concrete.

As seen in Figure3.2, ASR expansion at the end of exposure was approximately 4300 x 10^{-6} and no increase was observed from the age of 1150 days (about 3 years). This implies that expansion of used concrete almost finished. The same tendency was observed in the horizontal strain of the upper surface of the beam as seen in Fig.3.3. On the other hand, however, vertical strains in the side surfaces as well as upper longitudinal ones increased further from the age of 1150 days. This was mainly due to the increase in crack width of the existing expansive cracks (creep) caused by the eccentric chemical prestress. The influence of reinforcement corrosion on the increase in crack width was also considered. From the strain distribution in the cross section, the introduced chemical prestress was estimated and it became approximately 6.5 N/mm^2 at the bottom fibre.

3.1.2 Ultrasonic pulse velocity

In Figure 3.4 are shown the changes of ultrasonic pulse velocity in the beam during the exposure period. It is indicated that the value of the ultrasonic pulse velocity decreased to almost the half of its initial value at the age of about 1000 days. After that, however, the values restored at the end of exposure irrespective of the measured positions. The same tendency was also reported by Siegerd et al. [6]. From

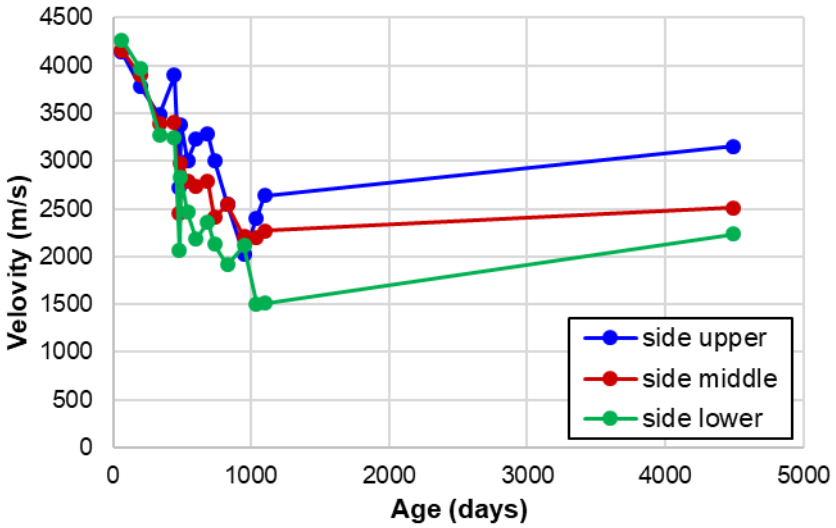

Figure 3.4: Changes in ultrasonic pulse velocity

this result, re-filling of micro cracks and pores by alkali-silica gel might occur. The value at the end of exposure became the largest in side upper and the smallest in side lower. This can be related to the density and the maximum width of expansive cracks depending on temperature, relative humidity, rainfall as well as local chemical prestress. Minute cracks were dominant in side upper white relatively wider ones were dominant in side lower, and this might led to the difference in re-filling by alkali-silica gel.

3.1.3 Mechanical properties of concrete

In Table 3.1 are listed the compressive strength and the elastic modulus of used concrete obtained from the test specimens (ϕ100mm x 200mm cylinders) exposed under the same condition as the beam. These values are the average ones obtained from at least 3 specimens, and significant scatter was not observed among those specimens.

The elastic modulus of the reactive concrete decreased remarkably at the age of 491 days. After that, however, its value began to increase again and almost restored at the end of exposure. This result coincided well with the tendency of the changes in ultrasonic pulse velocity.

Table3.1: Mecanical properties of concrete

Age (days)	Normal concrete		Reactive concrete	
	Compressive strength f'_c (N/mm^2)	Elastic modulus E_c (kN/mm^2)	Compressive strength f'_c (N/mm^2)	Elastic modulus E_c (kN/mm^2)
8	30.0	25.2	33.8	27.7
491	-	-	27.7	11.6
550	-	-	26.8	21.9
1150	28.2	24.9	26.5	25.4
4495	31.9	32.7	32.9	29.9

3.2 Results of beam loading test

3.2.1 Load carrying capacity and failure mode

Figure 3.5 shows the appearance of the beam after the loading test. In Table 3.2 are listed the measured maximum load and so on together with the calculated flexural and shear capacity according to the JSCE Standard Specifications for Concrete Structures [7], in which the mechanical properties of concrete at 4495 days were used and the material factors were set to be 1.0.

Figure 3.5: The appearance of the beam after the loading test

Table3.2: Results of loading test

Calculated		Measured			
Flexural capacity $P_{uf.cal}$ (kN)	Shear capacity $P_{us.cal}$ (kN)	Flexural cracking load $P_{cr.mea.}$ (kN)	Shear cracking load $P_{scr.mea.}$ (kN)	Maximum load $P_{u.mea.}$ (kN)	Failure mode
2189	1680	437	1300	2367	flexure

As indicated in Table 3.2, the beam failed finally in flexure although it was designed to fail in shear. This is mainly due to that the equation for estimation of shear capacity in JSCE Specifications is rather conservative and tends to underestimate the effect of prestress including chemical one. In addition, inspection after the loading test showed that rupture of stirrups did not occur during the exposure period, and this led to the preservation of shear capacity.

The measured maximum load well exceeded the calculated flexural capacity. However, the cover concrete in the compression zone of section peeled off in layers along with the existing expansive cracks at the ultimate state as seen in Figure 3.5. From these results, the design ultimate capacity of ASR damaged members might be guaranteed as long as no rupture occurs in tensile and shear reinforcements, although the final failure mode would be affected by the condition of existing cracks.

3.2.2 Deformation characteristics

Figure 3.6 shows the load – deflection relationships at the mid-span and the loading points. In Figure 3.7 are shown the relationship between the applied load and the maximum flexural and shear crack width. Flexural crack width was measured at the position of 35mm from the tension fibre in the mid-span region and shear one was measured at the mid-height of the section in the shear span on the line drawn from the loading point with 45 degrees against the vertical line.

As seen in Figure 3.6, the load – mid-span deflection curve turns out similar to the one which is observed typically in reinforced concrete members having an under-reinforced section.

Flexural cracks occurred at 437kN and the maximum crack width increased linearly until the yielding of tensile reinforcement. Although a shear crack occurred at around 1300kN and its width increased up to approximately 1.2mm, shear failure did not occur due to the effect of introduced chemical prestress. In addition, the no-ruptured stirrups, although their rupture had been expected during the exposure, performed well as shear reinforcement.

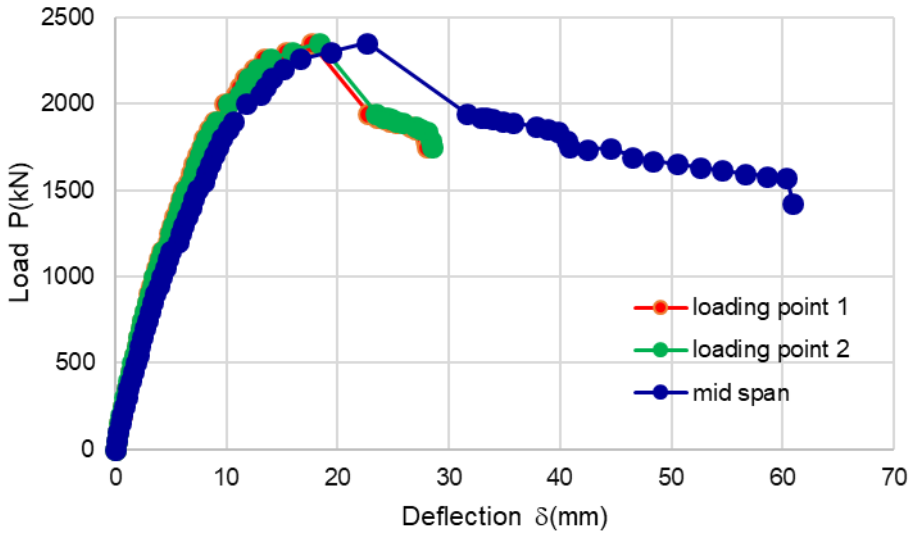

Figure 3.6: Load – deflection relationships

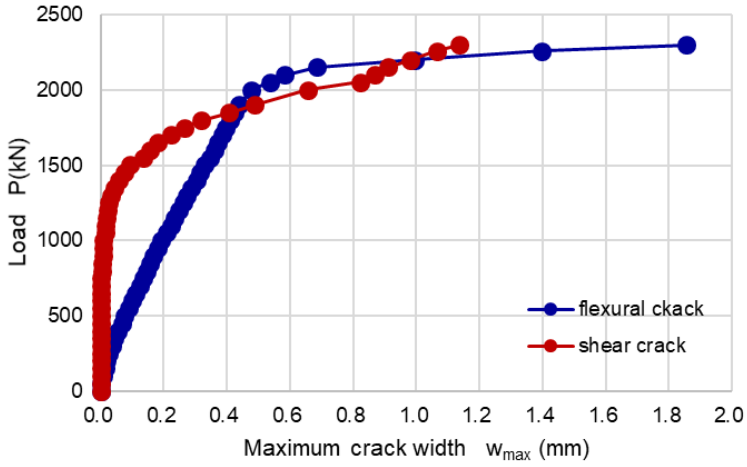

Figure 3.7: Load – maximum crack width relationships

3.3 Inspections after the loading test

3.3.1 Internal cracks

The beam was cut into 3 pieces after the loading test at the positions (700mm from both ends, see Figure 2.1) within the shear spans where the effect of loading test could be eliminated, and expansive crack propagation inside the concrete was observed. Figure 3.8 shows the internal cracking profiles of the sections.

As seen in Figure 3.8, relatively large cracks were observed in the concrete in the left and right inside sections. Large cracks were also observed at the position of the lower tensile reinforcement. These cracks connected with each other through the horizontal direction of the section. Except for these cracks, development of expansive cracks remained generally within the cover concrete outside the stirrups.

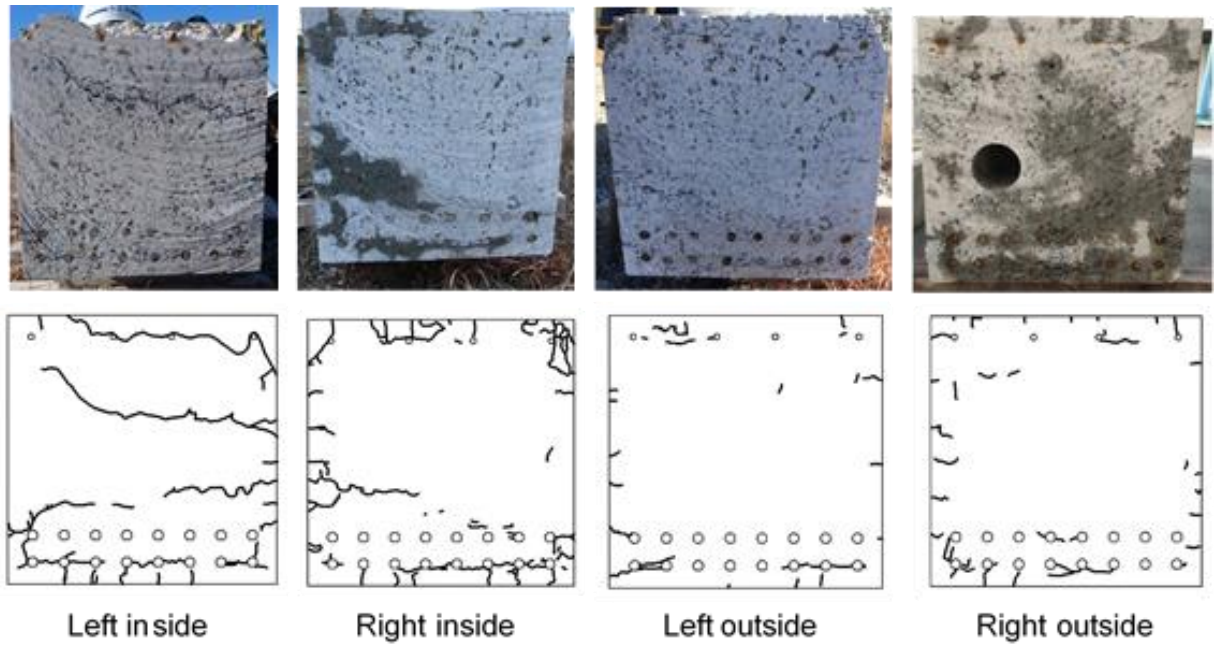

Figure 3.8: Cracking profiles inside the sections

3.3.2 Effect of anisotropy of ASR expansion on the properties of internal concrete

The effect of anisotropy of ASR expansion on the mechanical properties of internal concrete is examined by using concrete core specimens. These core specimens (ϕ 100mm cylinder) were taken from the

outside cut pieces of the beam in vertical, horizontal and longitudinal directions. The vertical specimens were taken from the top surface, while the other two were taken from the mid-height of the side surface and the cut surface, respectively. The number of specimens was three in each direction. Compressive strength and elastic modulus of these core specimens were measured. The average values of them are listed in Table 3.3.

Table3.3: Test results of concrete core specimens

Vertical		Horizontal		Longitudinal	
Compressive strength f'_c (N/mm^2)	Elastic modulus E_c (kN/mm^2)	Compressive strength f'_c (N/mm^2)	Elastic modulus E_c (kN/mm^2)	Compressive strength f'_c (N/mm^2)	Elastic modulus E_c (kN/mm^2)
18.2	12.2	14.5	5.75	17.5	9.04

As seen in Table 3.3, both of compressive strength and elastic modulus were the largest in vertical direction and the smallest in horizontal direction. However, these values were considerably smaller than those of the exposed specimens (see Table 3.1). This might be mainly due to the effect of released expansion of the core specimens as well as the inner cracks occurred during the loading test.

As for the effect of anisotropy of ASR expansion, definite difference was observed especially in the value of elastic modulus. The vertical specimens included the cover concrete of the top surface, in which ASR expansion almost finished as shown in Figure 3.3. On the other hand, the horizontal and longitudinal ones were taken from the mid-height of the section where the restraining of ASR expansion was relatively large, and this might result in larger released expansion especially in horizontal direction.

3.3.3 Condition of longitudinal bars and stirrups after the loading test

After the loading test, cover concrete in the mid-span region was tipped away and the condition of longitudinal bars and stirrups was observed. Figure 3.9 shows some profiles of the observed conditions.

As seen in Figure 3.9, longitudinal bars as well as stirrups corroded severely during the exposure due to the influence of NaCl which was added to obtain the prescribed total alkali contents. However, rupture of stirrups was not observed irrespective of the bending radius at the corners. One of this reason was that the shape of lugs and ribs of the used reinforcing bars was different from those of the ones used in the practical structures constructed more than several decades ago in which the rupture of them was detected. As shown in Table 3.2, the measured maximum flexural capacity exceeded well the design value and the final failure mode was flexure although shear was predicted. From these results, ASR expansion and reinforcement corrosion in the tested beam did not significantly affect the load carrying capacity.

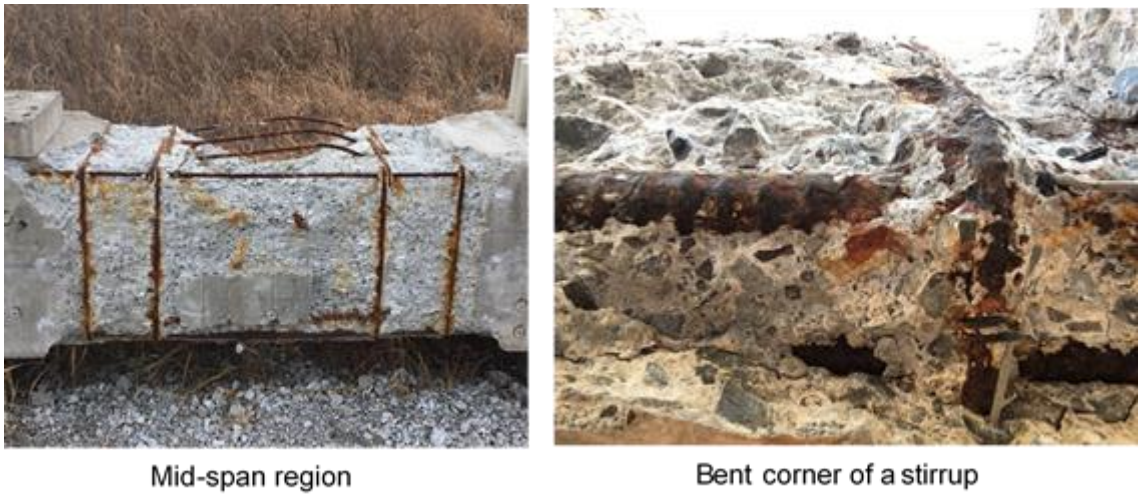

Figure 3.9: Condition of longitudinal bars and stirrups

4. CONCLUSIONS

In this study, ASR expansion characteristics in a relatively large scale reinforced concrete beam was investigated through the exposure of more than 12 years. Residual load carrying capacity was also examined by static loading test after the exposure. The main conclusions obtained are summarized as follows.

The expansive strain of the used reactive concrete increased up to approximately 4300×10^{-6} at the age of about 3 years. After that, however, the increase was not observed, and thus, the expansion of concrete almost finished at the age of about 12 years. The expansive strain in the tested beam showed different profiles according to the measuring position. The vertical strains in the side surfaces as well as the upper longitudinal ones increased further from the age of 1150 days while the horizontal strain in the upper surface showed the same tendency as that of the test pieces. This was mainly due to the increase in crack width of the existing expansive cracks caused by the eccentric chemical prestress. The influence of reinforcement corrosion on the increase in crack width was also considered. The estimated introduced chemical prestress was approximately 6.5 N/mm^2 at the bottom fibre of the section.

The elastic modulus of the reactive concrete test specimens decreased remarkably at the age of 491 days. After that, however, its value began to increase again and almost restored at the end of exposure. Similar tendency was observed in the changes in ultrasonic pulse velocity measured in the beam. This implies that re-filling of micro cracks and pores by alkali-silica gel might occur.

In the static loading test, the beam failed in flexure and its residual capacity exceeded well the design value although shear failure was predicted. This is mainly due to the conservativeness in the design equation for shear capacity and the effect of chemical prestress. In addition, rupture of stirrups did not occur during the exposure period, and this led to the preservation of shear capacity.

In the inspection after the loading test, a few relatively large expansive cracks were observed in the internal core concrete of the beam. Horizontal cracks at the position of the lower tensile reinforcement were also observed. Except for these cracks, the development of expansive cracks remained generally within the cover concrete. As for the effect of anisotropy of ASR expansion, definite difference was observed especially in the value of elastic modulus. This might be related to the released expansion of the concrete core specimens. In the core specimens taken from the direction and position where the restraint of expansion was relatively large, elastic modulus as well as compressive strength tended to show smaller values.

Although the rupture of stirrups was expected during the long-time exposure, no rupture occurred practically in spite of large expansion and relatively severe corrosion. Thus, the residual load carrying capacity of ASR damaged members might be guaranteed as long as the rupture of stirrups as well as tensile reinforcement did not occur.

5. REFERENCES

[1] Multon S, Seignol J-F and Toutlemonde F (2006) Chemomechanical Assessment of Beams Damaged by Alkali-Silica Reaction, Journal of Materials in Civil Engineering, ACSE, Vol.18, No.4, pp.500-509

[2] Japan Society of Civil Engineers (2005) State-of-the-Art Report on the Countermeasures for the Damage Due to Alkali-Silica Reaction, Concrete Library 124 (in Japanese)

[3] Inoue S, Oshita H, Sawai K and Hatano Y (2008) Effect of Rupture of Shear Reinforcement on Shear Capacity of ASR Damaged Reinforced Concrete Beams, Proc. of the 13th ICAAR

[4] Inoue S, Mikata Y, Takahashi Y, and Inamasu K (2012) Residual Shear Capacity of ASR Damaged Reinforced Concrete Beams with Ruptured Stirrups. Proc. of the 14th ICAAR

[5] Japanese Standards Association (2001) Method of test for alkali-silica reactivity of aggregates by chemical method, Japan Industrial Standards, JIS A 1145

[6] Siegert D, Multon S and Toutlemonde F (2005) Resonant Frequencies Monitoring of Alkali Aggregate Reaction (AAR) Damaged Concrete Beams, Experimental Techniques, Vol.29, No.6, pp.37-40

[7] Japan Society of Civil Engineers (2017) Standard Specifications for Concrete Structures – 2017, Design